

## Low Stimulated Brillouin Backscatter Observed from Large, Hot Plasmas in Gas-Filled Hohlräume

L. V. Powers, R. E. Turner, R. L. Kauffman, R. L. Berger, P. Amendt, C. A. Back, T. P. Bernat, S. N. Dixit, D. Eimerl, J. A. Harte, M. A. Henesian, D. H. Kalantar, B. F. Lasinski, B. J. MacGowan, D. S. Montgomery, D. H. Munro, D. M. Pennington, T. D. Shepard, G. F. Stone, L. J. Suter, and E. A. Williams

*Lawrence Livermore National Laboratory, Livermore, California 94551*

(Received 23 November 1994)

Stimulated Brillouin scattering (SBS) has been measured from hohlraums with plasma conditions similar to those predicted for high gain targets. The plasmas differ from the more familiar exploding foil or solid targets in being hot (3 keV), high electron density ( $10^{21}$  cm $^{-3}$ ), stationary, confined within a gold cylinder, and uniform over greater than 2 mm. Peak SBS backscatter is <3% in these hohlraums for an interaction beam with intensities of  $(1-4) \times 10^{15}$  W/cm $^2$ , laser wavelength equal to 0.351  $\mu$ m,  $f/4$  or  $f/8$  focusing optics, and a variety of beam smoothing implementations.

PACS numbers: 52.40.Nk, 52.50.Jm

The goal of inertial confinement fusion (ICF) is to produce energy by heating and compressing capsules containing fusion fuel. The proposed next-generation ICF facility, the National Ignition Facility (NIF), is designed to produce moderate energy gain from both x-ray heated ("indirect drive") and laser-heated ("direct drive") fuel capsules. Typical indirect drive targets consist of spherical fuel capsules enclosed in cylindrical gold hohlraums. Laser beams, arranged in cylindrical rings, heat the inside of the gold wall to produce x rays which in turn heat and implode the capsule to produce fusion conditions in the fuel. Detailed calculations show that adequate implosion symmetry is maintained by filling the hohlraum interior with low-density, low-Z gases [1]. The plasma produced from the heated gas provides sufficient pressure to keep the radiating gold surface from expanding excessively.

In the NIF targets, the laser beams will propagate through several millimeters of plasma with electron density of about  $10^{21}$  cm $^{-3}$  ( $n_e/n_c \sim 0.1$  for 0.351  $\mu$ m light) before depositing energy in the hohlraum wall. The fraction of the laser energy that is collisionally absorbed in the low-Z gas fill is modest ( $\sim 10\%$  at the peak of the laser pulse). However, estimates based on simple linear gain theory raise concern that stimulated Brillouin scattering (SBS) reflectivities could exceed acceptable levels of the large scale length plasmas in these targets. SBS reflectivity  $>10\%$  may unacceptably degrade target performance by reducing the energy available for radiation heating and/or disrupting symmetry. In the NIF plasmas, density and velocity gradients are weak, whereas damping of the SBS-produced ion waves by light ions in the gas fill is efficient [2] and limits the SBS gain coefficient. Under these conditions, the small signal intensity gain coefficient for SBS is

$$G_{\text{SBS}} = \pi \times 10^{-16} \left( \frac{I\lambda^2}{T_e} \right) \left( \frac{n_e}{n_c} \right) \left( \frac{\omega_a}{\nu_i} \right) \frac{L}{\lambda}, \quad (1)$$

where  $I$  is the laser intensity in W/cm $^2$ ,  $\lambda$  is the laser wavelength in microns,  $n_e/n_c$  is the electron density normalized to critical density,  $T_e$  is the electron temperature in keV,  $\omega_a$  and  $\nu_i$  are the ion-acoustic-wave frequency and amplitude damping rate, respectively, and  $L$  is the plasma length. Predicted gain coefficients for NIF plasmas are  $>20$ , whereas  $G_{\text{SBS}} < 15$  is required to ensure  $<10\%$  reflectivity if linear theory applies. (For such large gains theoretical estimates [3] indicate that nonlinear mechanisms will limit the scattering to lower levels.) Plasma conditions in past studies of parametric instabilities in laser-produced plasmas [4] differ significantly from expected NIF conditions. For those exploding foil or solid targets, where scale lengths  $\leq 1$  mm and electron temperatures  $\sim 0.5-2$  keV were typical, SBS is limited by detuning of the reflected light because of gradients in the flow velocity. The lack of quantitative theoretical understanding of those experiments discourages extrapolation to NIF conditions.

Random phase plates (RPP) [5] and temporal smoothing methods such as smoothing by spectral dispersion (SSD) [6] are commonly used in laser-plasma interaction experiments to increase the time-averaged beam uniformity at the target plane. Instability growth in an RPP intensity distribution [7] can vary with the size of the speckles. The role of speckles in determining instability levels is important for NIF because the underdense plasma size is large compared to the speckle size of the proposed  $f/8$  beam focusing. In simulations [8,9],  $f/8$  beams filament more than  $f/4$  beams. 3D simulations [10] show that SBS reflectivity, unlike filamentation, is not directly limited by the speckle length. In these simulations, SBS grows over the entire resonant region, which is several speckles long, with a total gain greater than that calculated for the average intensity. However, even if the bandwidth is less than the SBS growth rate, temporal smoothing reduces SBS by partially destroying the cooperative scattering among hot spots (phase conjugation). Modification of

the RPP intensity distribution by filamentation could also affect SBS. For the plasma parameters of these experiments and  $I \sim 2 \times 10^{15}$  W/cm<sup>2</sup>, simulations indicate that  $f/4$  speckles are stable to filamentation but  $f/8$  speckles are unstable [9]. Temporal smoothing makes filamentation more difficult because the filament must form before the hot spot moves to a different location. One goal of these experiments is to test the  $f$  number and temporal smoothing scaling of SBS.

We have used the Nova laser to produce plasmas with conditions similar to those predicted for NIF hohlraum targets and have measured SBS from these plasmas. In these experiments, the targets are cylindrical gold hohlraums with length and diameter of 2.5 mm [11]. The hohlraums do not contain capsules, but are filled with neopentane (C<sub>5</sub>H<sub>12</sub>) gas at a pressure of 1 atm ( $10^{21}$  electrons/cm<sup>3</sup> when fully ionized). As shown in Fig. 1, the gas is contained by two polyimide (C<sub>22</sub>H<sub>10</sub>N<sub>2</sub>O<sub>5</sub>) windows  $\sim 6500$  Å thick. Nine beams of Nova in two rings heat the gas with  $\sim 30$  kJ of 0.351  $\mu$ m light in a 1.4 ns shaped pulse. The tenth beam is a probe, or interaction, beam whose intensity, pulse shape,  $f$  number, and “smoothness” are varied. The SBS backscatter intensity and spectrum from the interaction beam are measured with time resolution of 100 ps and spectral resolution of 1 Å. The interaction beam has a trapezoidal pulse with an  $\sim 600$  ps flattop and an  $\sim 300$  ps rise and fall. The interaction beam is typically delayed  $\sim 600$  ps relative to the start of the heating beams, and is smoothed spatially with a RPP providing intensities in the range of  $(1-4) \times 10^{15}$  W/cm<sup>2</sup> at the peak of the Airy pattern. Temporal smoothing is done either by SSD with frequency modulation bandwidth [6] or by 4 colors [12]. The 4-color scheme propagates four frequencies through four quadrants of the focusing lens and overlaps them at the focal plane. The line separation is  $\delta\lambda = 4.4$  Å at 1.053  $\mu$ m for a total linewidth of 13.2 Å for these experiments (4-color bandwidth with  $\delta\lambda \cong 10$  Å is proposed for the NIF).

To produce a uniformly hot plasma inside the Nova hohlraum, a substantial fraction of Nova’s energy ( $\sim 12$  kJ) must be coupled to the gas. Because the absorption length exceeds the target size for the temperatures of interest

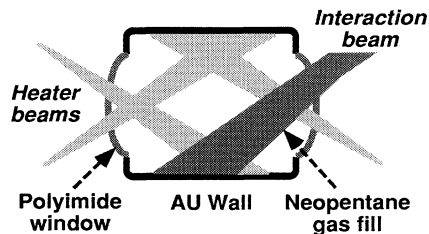


FIG. 1. Schematic diagram of the target geometry. Shaded regions show the focusing and pointing of the heater beams (light shading) and interaction beam (dark shading).

(>5 mm for 0.351  $\mu$ m light at  $T_e = 3$  keV), the energy absorbed in the gas is determined by the laser path length. The heater beam geometry shown in Fig. 1 was chosen to produce the desired plasma temperature by maximizing the absorption in the gas. We also use a ramped pulse for the heater beams to avoid scattering from the solid window material or the initially cold fill gas. The detailed plasma conditions for both the Nova gas-filled hohlraums and NIF targets are obtained from 2-dimensional LASNEX [13] simulations. The simulations are cylindrically symmetric about the hohlraum axis, and include the gold hohlraum wall, the gas fill (including dopants in the Nova targets), the membrane over the laser entrance hole which confines the gas, and (in the case of the NIF target) the capsule. Standard LASNEX models are used for Lagrangian hydrodynamics, laser absorption, radiation transport, flux limited electron transport (using  $f = 0.05$ ), and nonlinear thermal equilibrium atomic physics. The simulations predict that a uniform plasma  $\sim 2$  mm long with electron density  $\sim 10^{21}$ /cm<sup>3</sup>, electron temperature  $\sim 3$  keV, and flow velocity  $< 10^7$  cm/sec is maintained for  $> 0.5$  ns during the peak of the interaction pulse. A more extensive description of the plasma conditions and LASNEX simulations will be published elsewhere.

To illustrate the similarity between plasma conditions in NIF target designs and Nova gas-filled hohlraums, we summarize in Table I the SBS gain and the calculated values of the plasma parameters in the underdense plasma that determine the gain.

The Nova plasma parameters are within  $\sim 50\%$  of the NIF values except for the ion/electron temperature ratio, which is lower in the Nova targets because of the shorter time available for electron-ion equilibration to occur. This difference leads to larger ion acoustic wave damping  $\nu_i$  in NIF than in Nova targets [2]. However, the difference in path length compensates to give similar gain coefficients for NIF and Nova targets in the same intensity ( $I \cong 2 \times 10^{15}$  W/cm<sup>2</sup>). Hence these Nova targets access conditions that are very similar to NIF designs both in SBS linear gain and in the individual plasma parameters that determine the scattering characteristics. Calculated gain coefficients for the highest intensity Nova experiments ( $I \cong 5 \times 10^{15}$  W/cm<sup>2</sup>) exceed the NIF value by more than a factor of 2.

TABLE I. Comparison of selected plasma parameters for Nova gas-filled hohlraums and NIF targets.

	Nova	NIF
Interaction length $\int dl$	$\sim 2$ mm	$\sim 3$ mm
Line density $\int (n_e/n_c) dl$	$\sim 0.2$ mm	$\sim 0.3$ mm
Electron temperature	3 keV	5 keV
Ion/electron temperature ratio	0.1–0.2	0.4
Gain coefficient $G_{\text{SBS}}$ ( $2 \times 10^{15}$ W/cm <sup>2</sup> )	22	21

Extensive characterization has been carried out to assure that predicted plasma conditions have been achieved in the underdense plasma. The electron temperature is inferred from both single-element and isoelectric line ratios [14] from Ti/Cr or K/Cl spectra from foils placed in the path of the interaction beam. Detailed analysis of the isoelectronic spectra confirms that  $T_e > 3$  keV during the interaction pulse [15]. Time-resolved measurements without the interaction beam verify that electron conduction provides good temperature uniformity. Several diagnostics characterize the propagation of the heating beams through the (initially) cold gas. The temporal history of gold  $M$ -band emission from streaked spectra recorded through the laser entrance hole provides a measure of the beam propagation speed in the gas. Gated x-ray images, dominated by emission from 1% Ar dopant in the gas, provide evidence that the beams propagate without significant breakup or refraction. These experimental observations, which are in good agreement with LASNEX predictions, support important aspects of our modeling of NIF targets.

Backscattered light near the laser frequency is measured with a grating spectrometer–streak-camera combination as well as with time-integrating calorimeters. Spectra recorded from each of the four quadrants of the lens show the same temporal evolution and spectral shift relative to the incident frequency in that quadrant. A typical backscattered spectrum is shown in Fig. 2. Reflection from the expanding window at the laser entrance hole produces the unshifted feature in time-resolved spectra early in the interaction pulse. The reflectivity peaks soon after

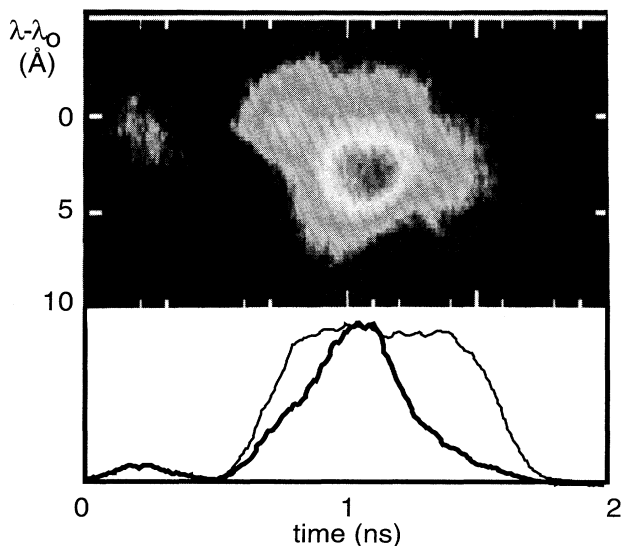


FIG. 2. Streaked spectrum of backscattered light from 1-color  $f/8$  interaction beam. Temporal lineouts of the frequency-integrated reflectivity (bold line) and the interaction beam intensity (light line) are plotted below. The peak reflectivity is 0.015 and the peak intensity is  $I = 1.7 \times 10^{15}$  W/cm<sup>2</sup> for this case.

the interaction beam reaches peak intensity and decreases before the intensity drops. We calculate that this time dependence results from a decrease in the gain caused by an increase in the ion acoustic wave damping rate as the ion-electron temperature ratio increases in time. At the time of peak scattering, the wavelength of the peak emission is redshifted  $\sim 3$ – $7$  Å. In the fluid limit, the frequency shift of SBS scattered light is  $\Delta\omega = 2k_0(V_{\parallel} - C_s)$ , where  $k_0$  is the laser wave number,  $C_s$  is the ion sound speed, and  $V_{\parallel}$  is the flow velocity parallel to the scattering vector; hence the observed redshift is evidence that the SBS spectrum is dominated by scattering from regions of plasma where  $V_{\parallel} < C_s$  as predicted by linear gain analysis. By contrast, SBS spectra from lower temperature, expanding targets [4] are routinely blueshifted.

Figure 3 shows the peak SBS backscatter into the lens as a function of intensity for  $f/4$  and  $f/8$  interaction beams. Peak SBS reflectivities with  $f/8$  interaction beams, which closely match the NIF beam configuration, are  $< 3\%$  for neopentane-filled targets. Time-integrated reflectivities are less than 1%. The scattering levels for all intensities are well below the  $> 30\%$  reflectivities predicted by linear theory. Reflectivity levels are not changed when 4-color bandwidth is added. This insensitivity to bandwidth agrees with simulations [10] on if *ad hoc* nonlinear damping rates are imposed to match the measured SBS reflectivity. At higher interaction intensities ( $> 2 \times 10^{15}$  W/cm<sup>2</sup>), the simulations indicate that filaments form and scatter significant light outside the lens cone. Estimates of the angular distribution of the backscattered light based on energy collected by photodiodes near the backscatter direction indicate that the total backscatter is within a factor of 2 of the backscatter into the lens for these

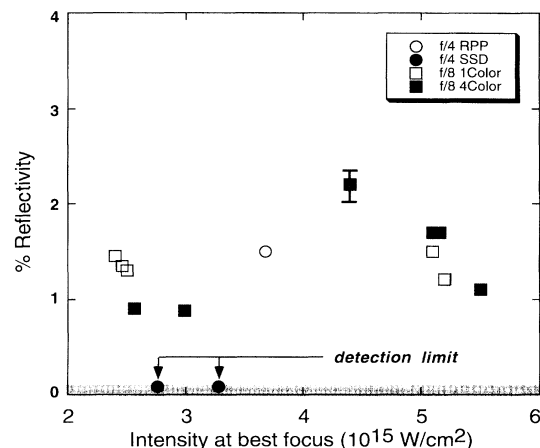


FIG. 3. SBS reflectivity into the focusing lens for  $f/4$  (circles) and  $f/8$  (squares) interaction beams. Filled squares show  $f/8$  shots for which 4-color bandwidth with  $4.4$  Å line separation was added. Reflectivities from  $f/4$  shots with  $3.5$  Å SSD bandwidth (filled circles) were below the detection threshold.

experiments. More detailed measurements of the angular distribution of the reflected light are now underway.

Peak scattering levels from  $f/4$  interaction beams are comparable to  $f/8$  (1%–2%). With an SSD bandwidth of 3.5 Å, scattering from the interaction beam is below the detection threshold of ~0.1%. The apparent efficiency of SSD in suppressing SBS may be related to the details of the speckle motion: with SSD, the hot spots move in an effectively random way, whereas with 4-color smoothing the hot spot pattern exactly recurs in a time  $2\pi/\delta\omega$ , where  $\delta\omega$  is the line separation.

The observation of similar reflectivities from single-color  $f/4$  and  $f/8$  interaction beams at comparable nominal intensities is somewhat at odds with gain scaling. For these large plasmas, beam divergence produces a significant drop in intensity (a factor of ~2 for  $f/8$  and ~4 for  $f/4$ ) across the scattering region. This difference leads to a larger calculated gain for  $f/8$  ( $G_{\text{SBS}} = 22$ ) than for  $f/4$  ( $G_{\text{SBS}} = 15$ ) for the same intensity at best focus. Several possible explanations for these findings are under investigation theoretically and experimentally. For example, for the large gains calculated for these targets, nonlinear saturation mechanisms may limit the amplitude of the ion waves driven by SBS [3]. The measured energy in hot electrons for these experiments is <1% of the incident laser energy in all cases indicating that stimulated Raman scattering is low, in agreement with linear gain estimates.

We have demonstrated low SBS reflectivity in NIF-relevant gas-filled hohlraum experiments on Nova. These targets closely match the calculated plasma conditions and SBS gain coefficients for NIF targets. The interaction beam mimics the NIF laser beam intensity, focusing, and beam smoothing. The maximum time-dependent SBS reflectivity is less than 3% for NIF-relevant conditions.

The authors acknowledge valuable discussions with J. Kilkenny, J. Lindl, and M. Rosen of LLNL and J. Fernandez, W. Hsing, and B. Wilde of LANL. The contributions of the Nova laser operations and target fabrication groups were indispensable in conducting these experiments. Polyimide membranes were fabricated by Luxel Corporation. We acknowledge the LASNEX group for making possible the simulations required to design and analyze these experiments. This work was performed under the auspices of the U.S. DOE by Lawrence Livermore National Laboratory under Contract No. W-7405-Eng-48.

- [1] S. W. Haan, S. M. Pollaine, J. D. Lindl, L. J. Suter, L. V. Powers, R. L. Berger, E. Alley, G. Zimmerman, P. A. Amendt, W. K. Levedahl, R. A. Sacks, A. I. Shestakov, G. L. Strobel, S. Weber, W. Krauser, N. M. Hoffman, D. Wilson, and D. Harris (to be published).
- [2] E. A. Williams, R. L. Berger, A. V. Rubenchik, R. P. Drake, B. S. Bauer, D. D. Meyerhofer, and T. W. Johnston (to be published).
- [3] W. L. Kruer, *Phys. Fluids* **23**, 1273 (1980).
- [4] H. A. Baldis, D. S. Montgomery, J. D. Moody, C. Labaune, S. H. Batha, K. G. Estabrook, R. L. Berger, and W. L. Kruer, *Plasma Phys. Controlled Fusion* **34**, 2077 (1992), and references therein.
- [5] Y. Kato and K. Mima, *Appl. Phys. B* **29**, 186 (1982).
- [6] S. Skupsky, R. W. Short, T. Kessler, R. S. Craxton, S. Letzring, and J. M. Soures, *J. Appl. Phys.* **66**, 3456 (1989).
- [7] S. N. Dixit, I. M. Thomas, B. W. Woods, A. J. Morgan, M. A. Henesian, P. J. Wegner, and H. T. Powell, *Appl. Opt.* **32**, 2543 (1993).
- [8] Andrew J. Schmitt, *Phys. Fluids* **31**, 3079 (1988).
- [9] R. L. Berger, B. F. Lasinski, T. B. Kaiser, E. A. Williams, A. B. Langdon, and B. I. Cohen, *Phys. Fluids B* **5**, 2243 (1993).
- [10] R. L. Berger, *Bull. Am. Phys. Soc.* **38**, 2012 (1993).
- [11] This target geometry was one of three simultaneous and complementary experiments with Nova using gas-filled targets to create large scale length plasmas. Experiments using targets in which the gas is contained in a low-Z membrane are reported by B. J. MacGowan *et al.*, in *Proceedings of the International Atomic Energy Agency 15th International Conference on Plasma Physics and Controlled Nuclear Fusion Research* (IAEA, Vienna, 1994). An alternate hohlraum geometry was fielded by a team from Los Alamos National Laboratory led by J. Fernandez.
- [12] D. M. Pennington, M. A. Henesian, R. B. Wilcox, T. L. Weiland, R. B. Ehrlich, C. W. Laumann, D. Eimerl, and H. T. Powell, *Tech. Dig.* **8**, 161 (1994).
- [13] G. Zimmerman and W. Kruer, *Comments Plasma Phys. Controlled Fusion* **2**, 85 (1975).
- [14] R. S. Majoribanks, M. C. Richardson, P. A. Jaanimagi, and R. Epstein, *Phys. Rev. A* **46**, 1747 (1992).
- [15] C. A. Back, E. J. Hsieh, R. L. Kauffman, D. H. Kalantar, D. E. Klem, R. W. Lee, B. J. MacGowan, D. S. Montgomery, L. V. Powers, T. D. Shepard, L. J. Suter, G. F. Stone, and R. E. Turner (to be published).

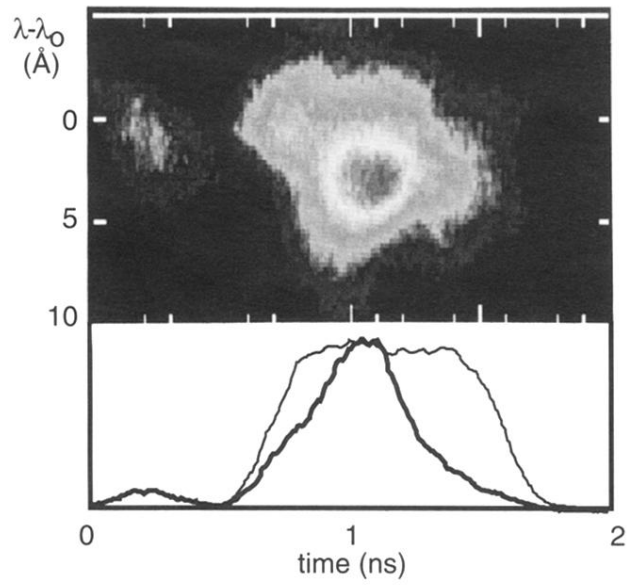


FIG. 2. Streaked spectrum of backscattered light from 1-color  $f/8$  interaction beam. Temporal lineouts of the frequency-integrated reflectivity (bold line) and the interaction beam intensity (light line) are plotted below. The peak reflectivity is 0.015 and the peak intensity is  $I = 1.7 \times 10^{15}$  W/cm<sup>2</sup> for this case.